Supporting Information (SI)

Hybrid Composites of Lanthanide Metal-Organic Frameworks with Epoxy Silanes for Highly Sensitive Thermometry

Ying Shu,[a] Huiru Guan,[a] Alexander M. Kirillov,[b] Weisheng Liu,[a] Lizi Yang*[a] Wei Dou*[a]

[a]State Key Laboratory of Applied Organic Chemistry and Key Laboratory of Nonferrous Metals Chemistry and Resources Utilization of Gansu Province, College of Chemistry and Chemical Engineering, Lanzhou University, Lanzhou 730000, P. R. China;

[b]Centro de Química Estrutural, Institute of Molecular Sciences, Departamento de Engenharia Química, Instituto Superior Técnico, Universidade de Lisboa, Av. Rovisco Pais, 1049-001, Lisbon, Portugal.

SI contains: Supporting Figures S1−S15 and Tables S1−S3 with additional data on characterization, properties, and application of Ln-MOFs and Ln-MOF@Epoxy composites.

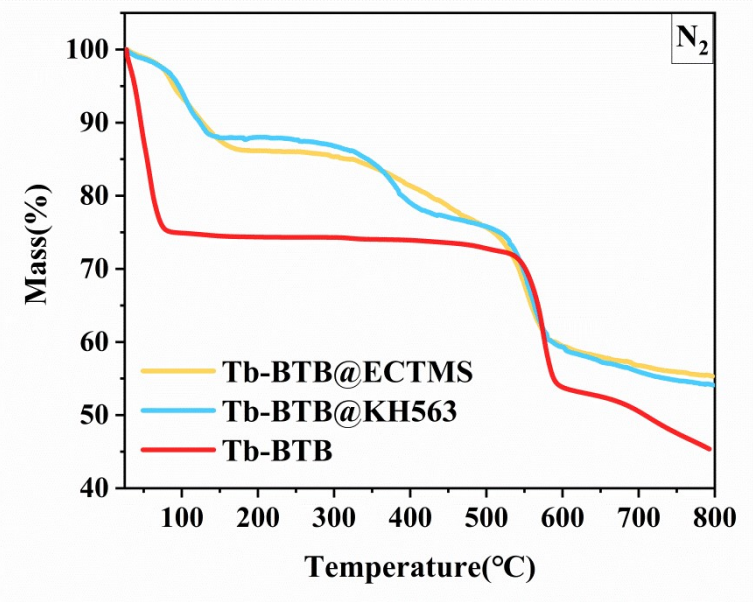

Figure S1. TGA profiles for Tb-BTB, Tb-BTB@KH563, and Tb-BTB@ECTMS under N_2 atmosphere.

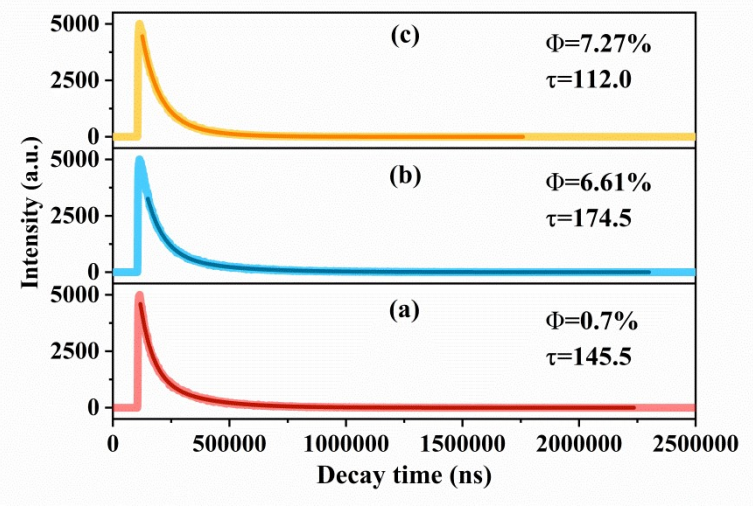

Figure S2. Luminescence decay curve for (a) Tb-BTB, (b) Tb-BTB@KH563, and (c) Tb-BTB@ECTMS at room temperature (λ_{ex} = 322 nm).

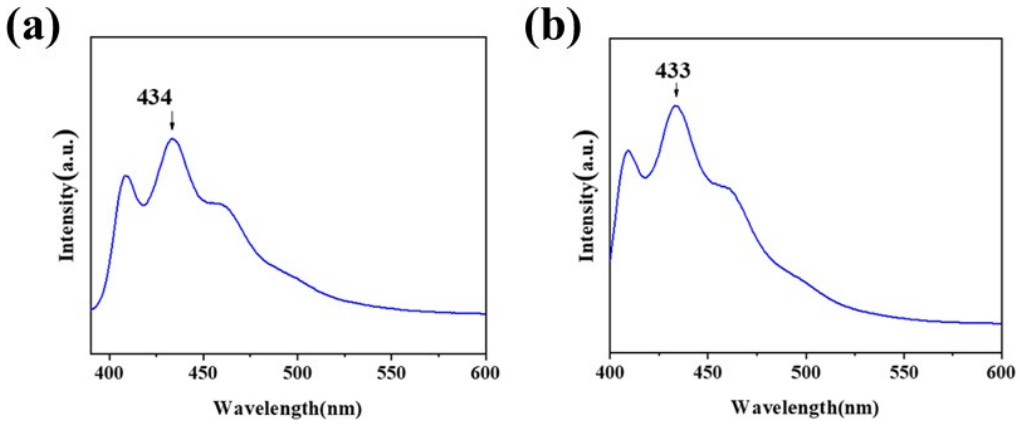

Figure S3. Liquid-state emission spectra of (a) ECTMS and (b) KH563.

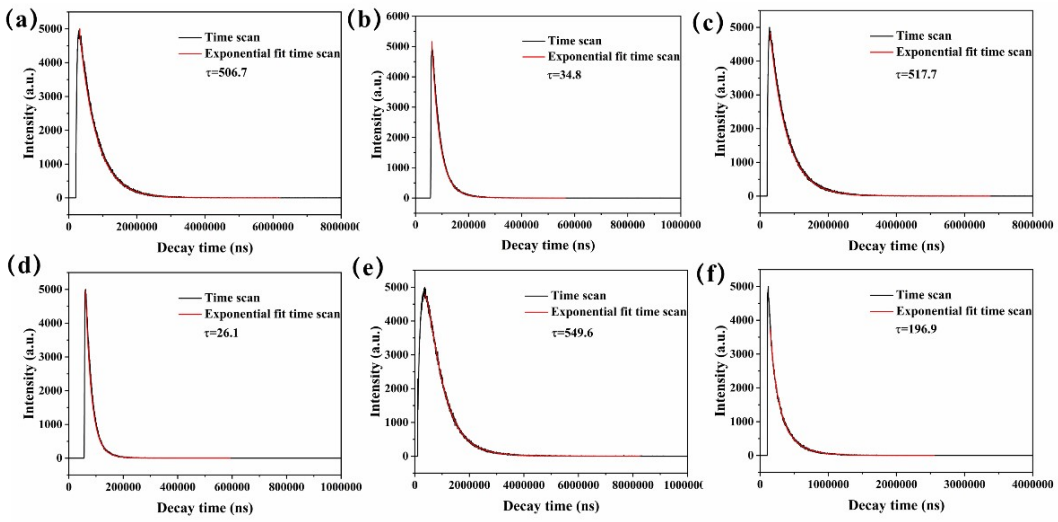

Figure S4. Luminescence decay curves of $Eu_{0.001}Tb_{0.999}$-BTB: (a) $^5D_0$ (Eu^{3+}, monitored at 613 nm) and (b) $^5D_4$ (Tb^{3+}, monitored at 546 nm). Luminescence decay curves of $Eu_{0.001}Tb_{0.999}$-BTB@ECTMS: (c) $^5D_0$ (Eu^{3+}, monitored at 613 nm) and (d) $^5D_4$ (Tb^{3+}, monitored at 546 nm). Luminescence decay curves of $Eu_{0.001}Tb_{0.999}$-BTB@KH563: (e) $^5D_0$ (Eu^{3+}, monitored at 613 nm) and (f) $^5D_4$ (Tb^{3+}, monitored at 546 nm). All curves were measured at room temperature.

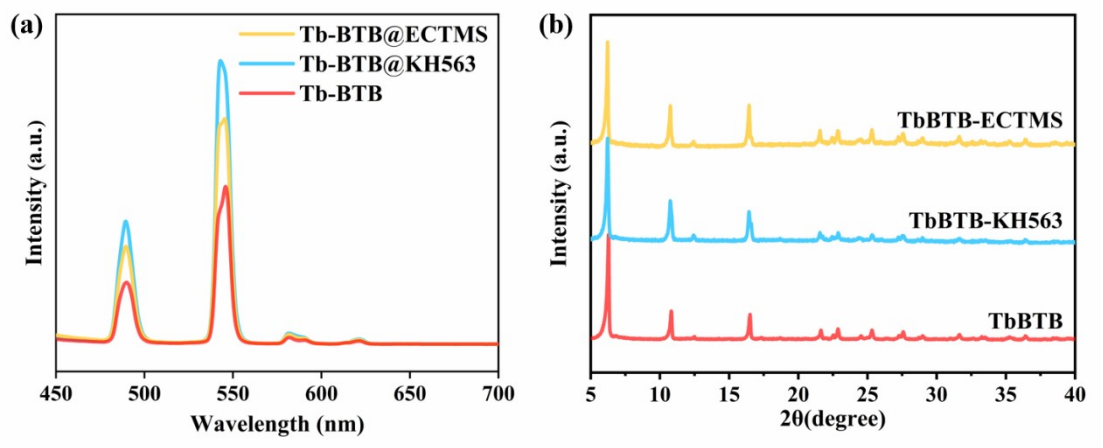

Figure S5. (a) Solid-state emission spectra (λ_{ex} = 322 nm) and (b) PXRD patterns of Tb-BTB, Tb-BTB@KH563, and Tb-BTB@ECTMS after 24 h in boiling water.

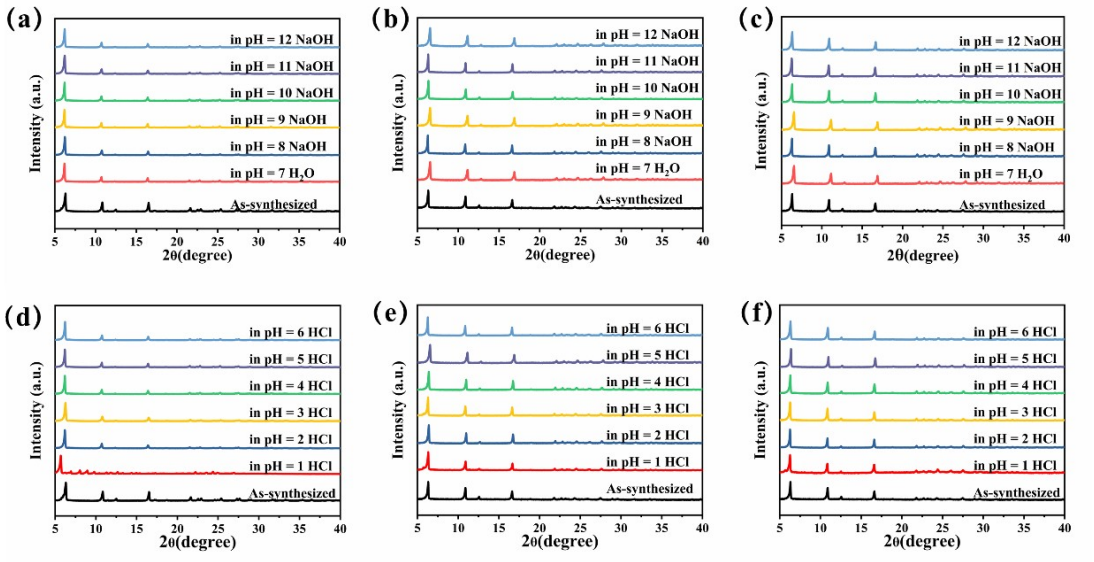

Figure S6. PXRD patterns of (a,d) Tb-BTB, (b,e) Tb-BTB@KH563, and (c,f) Tb-BTB@ECTMS after stability tests for 1 h in aqueous solutions at different pH (1–12).

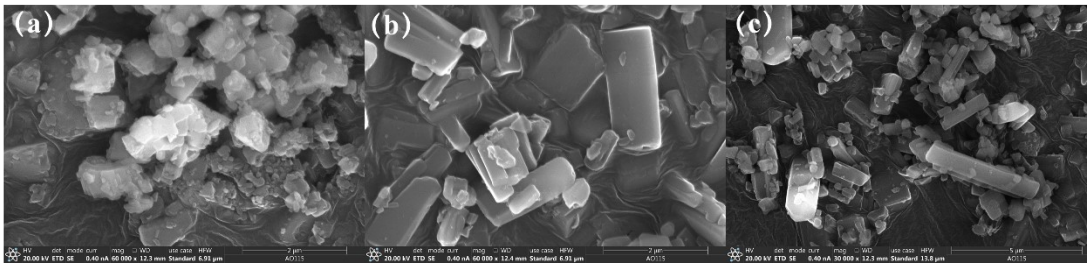

Figure S7. SEM morphology of (a) Tb-BTB, (b) Tb-BTB@KH563, and (c) Tb-BTB@ECTMS after stability tests in boiling water for 24 h.

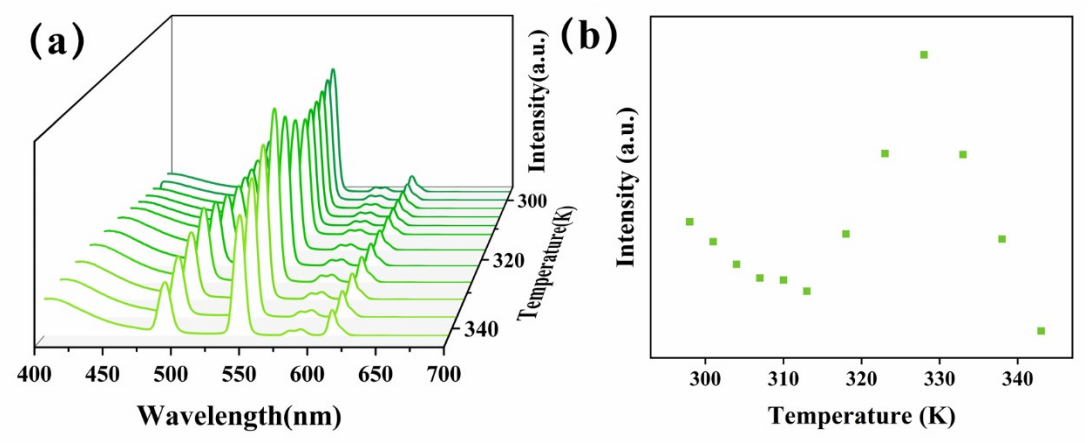

Figure S8. (a) Emission spectra of Tb-BTB recorded between 298 and 343 K. (b) The emission intensity of the $^5D_4 \rightarrow {}^7F_5$ transition in Tb-BTB at different temperatures (298-343 K).

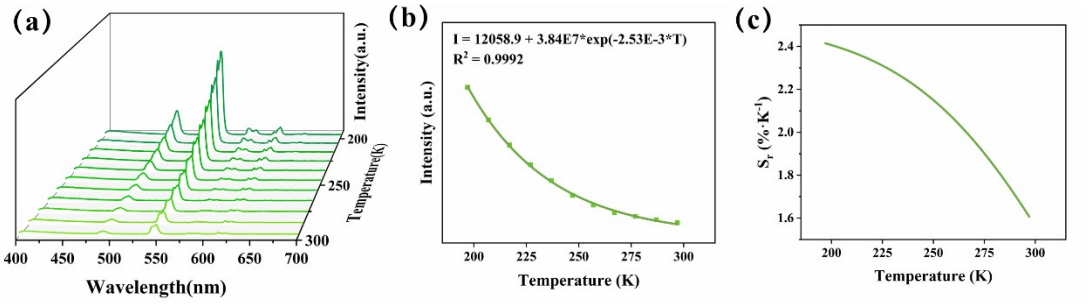

Figure S9. (a) Emission spectra of Tb-BTB recorded between 197 and 297 K. (b) Emission intensity of the $^5D_4 \rightarrow {}^7F_5$ transition in Tb-BTB at different temperatures (197-297 K). (c) Relative sensitivity of Tb-BTB in the 197-297 K range.

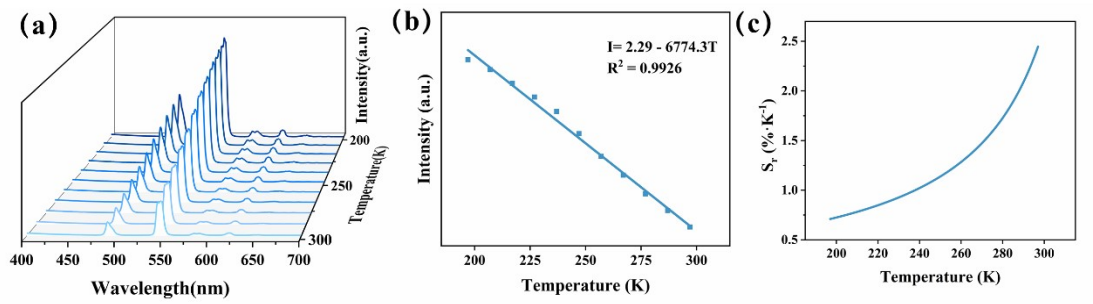

Figure S10. (a) Emission spectra of Tb-BTB@ECTMS recorded between 197 and 297 K. (b) Emission intensity of the $^5D_4 \rightarrow {}^7F_5$ transition in Tb-BTB@ECTMS at different temperatures (197-297 K). (c) Relative sensitivity of Tb-BTB@ECTMS in the 197-297 K range.

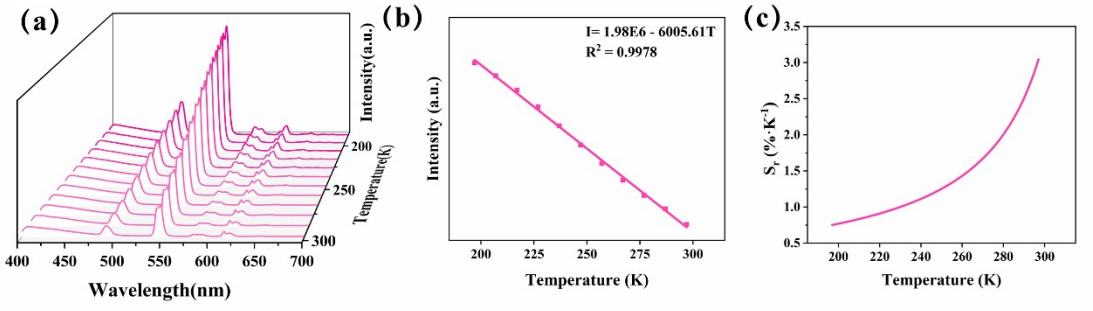

Figure S11. (a) Emission spectra of Tb-BTB@KH563 recorded between 197 and 297 K. (b) Emission intensity of the $^5D_4 \rightarrow {}^7F_5$ transition in Tb-BTB@KH563 at different temperatures (197-297 K). (c) Relative sensitivity of Tb-BTB@KH563 in the 197-297 K range.

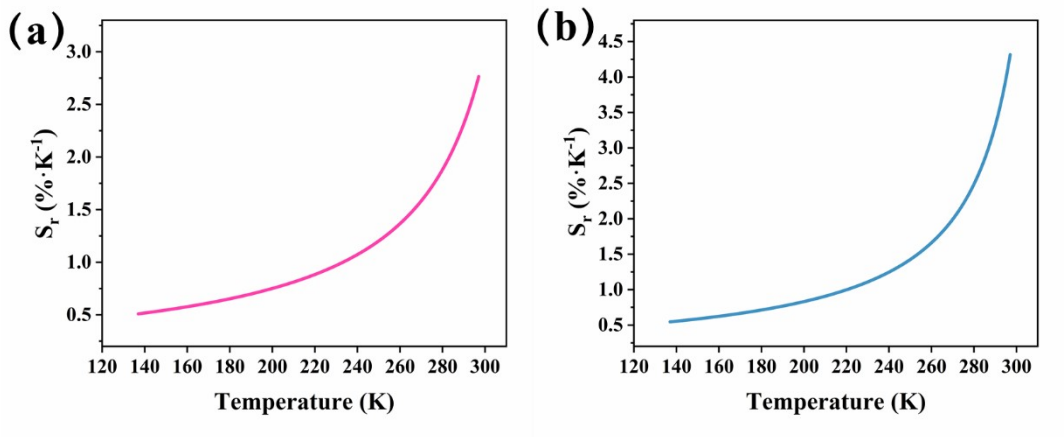

Figure S12. (a) Relative sensitivity of $Eu_{0.001}Tb_{0.999}$-BTB@KH563 in the 137-297 K range. (b) Relative sensitivity of $Eu_{0.001}Tb_{0.999}$-BTB@ECTMS in the 137-297 K range.

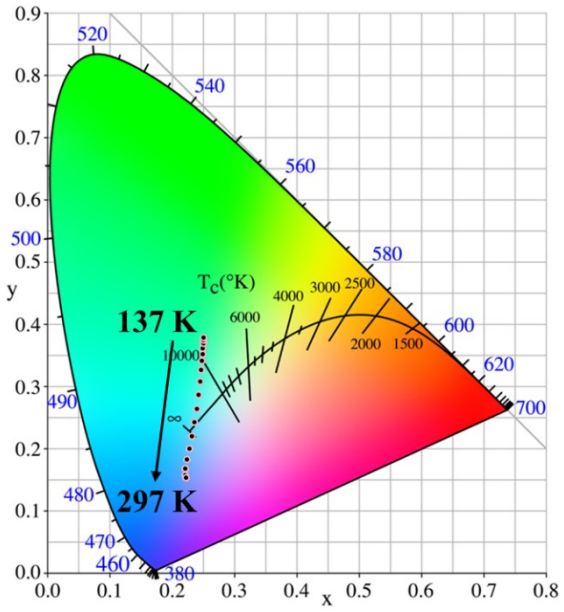

Figure S13. CIE chromaticity diagram of $Eu_{0.001}Tb_{0.999}$-BTB@ECTMS at different temperatures under 323 nm excitation.

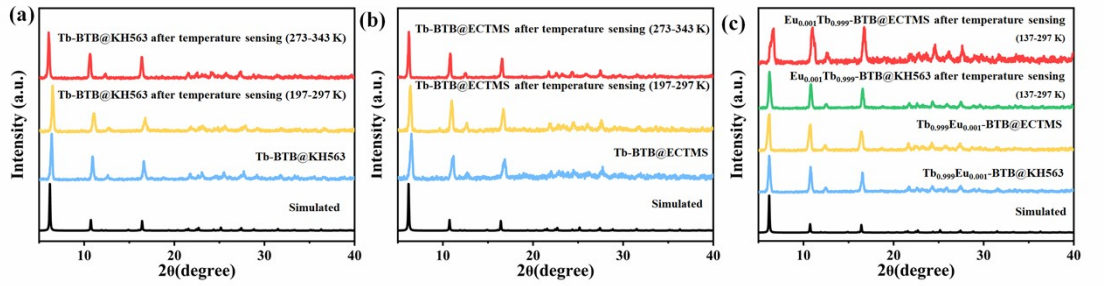

Figure S14. PXRD patterns of (a) Tb-BTB@KH563, (b) Tb-BTB@ECTMS, (c) $Eu_{0.001}Tb_{0.999}$-BTB@KH563 and $Eu_{0.001}Tb_{0.999}$-BTB@ECTMS after temperature sensing.

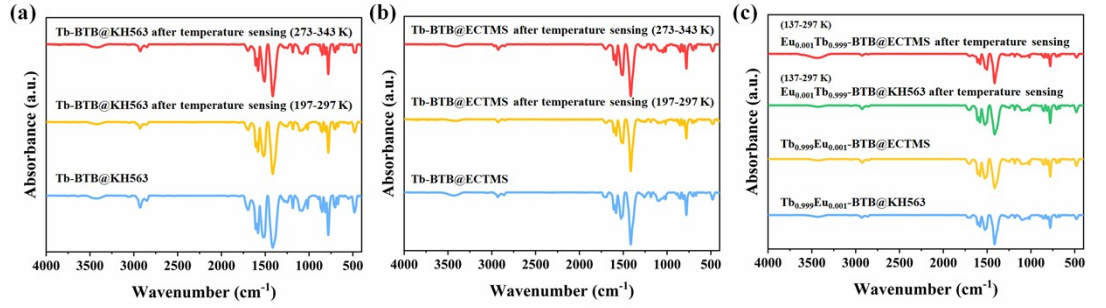

Figure S15. FTIR spectra of (a) Tb-BTB@KH563, (b) Tb-BTB@ECTMS, (c) $Eu_{0.001}Tb_{0.999}$-BTB@KH563 and $Eu_{0.001}Tb_{0.999}$-BTB@ECTMS after temperature sensing.

Table S1. The detailed ICP studies of Ln-MOF and Ln-MOF@Epoxy.

Sample	Test element	Concentration (mg/L)	Mass ratio (Ln-BTB:Epoxy)	Molar ratio (Eu:Tb)
Tb-BTB@KH563	**Tb**	**29.66**	**0.034**	
	Si	**0.60**		
Tb-BTB@ECTMS	**Tb**	**15.50**	**0.064**	
	Si	**0.58**		
$Tb_{0.999}Eu_{0.001}$-BTB@KH563	**Tb**	**0.042**	**0.030**	**0.0011**
	Eu	**0.042**		
	Si	**0.58**		
$Tb_{0.999}Eu_{0.001}$-BTB@ECTMS	**Tb**	**34.71**	**0.054**	**0.0013**
	Eu	**0.038**		
	Si	**1.12**		

Table S2. Fluorescence lifetimes for Ln-MOF and Ln-MOF@Epoxy in the solid-state.[a]

Sample		Initial τ (μs)	After grafting with ECTMS τ (μs)	After grafting with H563 τ (μs)
Tb-BTB		**145.5**	**112**	**174.5**
$Eu_{0.001}Tb_{0.999}$-BTB	**Eu**	**506.7**	**517.7**	**549.6**
	Tb	**34.8**	**26.1**	**196.9**

[a] Samples were tested at room temperature.

Table S3. Fluorescence quantum yield data for Ln-MOF and Ln-MOF@Epoxy in the solid-state.[a]

Sample	Initial ϕ (%)	After grafting with ECTMS ϕ (%)	After grafting with KH563 ϕ (%)
Tb-BTB	**0.7**	**7.27**	**6.61**
$Eu_{0.001}Tb_{0.999}$-BTB	**0.67**	**8.69**	**5.13**

[a] Samples were tested at room temperature; ϕ is the absolute quantum yield.

Table S4. Temperature sensing data for Ln-MOF and Ln-MOF@Epoxy: working ranges (K), maximum relative sensitivity values (S_m, % K^{-1}), and equations.

Sample	Range (K)	S_m (% K^{-1})	Equation
Tb-BTB	**197-297**	**2.41**	**I = 12058.9 + 3.84E7 * exp (-2.53E-3 * T)**
Tb-BTB@KH563	**273-343**	**6.18**	**I = 5.174E6 - 14405.07 * T**
	197-297	**3.04**	**I = 1.98E6 - 6005.61 * T**
Tb-BTB@ECTMS	**273-343**	**6.85**	**I = 5.798E6 - 16214.88 * T**
	197-297	**2.45**	**I = 2.29 - 6774.3 * T**
$Tb_{0.999}Eu_{0.001}$-BTB@ECTMS	**137-297**	**4.32**	**Δ = 12.8089 - 0.04 * T**
$Tb_{0.999}Eu_{0.001}$-BTB@KH563	**137-297**	**2.76**	**Δ = 9.7847 - 0.0294 * T**